Dielectrics Newsletter

Scientific newsletter for dielectric and impedance spectroscopy Issue July 2020

Dielectric spectroscopy of nonlinear effects

Ranko Richert

A typical result of a dielectric relaxation experiment is reported as the frequency dependent permittivity, ε, where ε(ω) is derived from polarization P and electric field E via $\varepsilon = 1 + \chi$ and $\chi = P/(\varepsilon_0 E)$ [1]. In many cases, the level of the electric field used to determine ε is not reported, and the justification for this feature is that permittivity is independent of the field over a large range, because P is often proportional to E for fields not exceeding 10 kV/cm. If the entire loss spectrum, ε''(ω), remains field invariant, this implies that quantities such as relaxation amplitude $\Delta\varepsilon=\varepsilon_s-\varepsilon_\infty$ or relaxation time constant τ_D are not affected by the magnitude of the electric field.

This independence of the field amplitude changes when higher electric fields are applied, say $E \geq 100$kV/cm. Historically, the first non-linear dielectric effect that was studied systematically was that of dielectric saturation, the reduction of the relaxation amplitude by the fact that the polarization is bounded by the limiting orientation, where the average cosine of the angle between dipole moment μ and field E reaches its highest value, $\langle\cos\theta\rangle = 1$. Debye has predicted this effect on the basis of the Langevin function, $\langle\cos\theta\rangle \approx a/3 - a^3/45$, where $a = \mu E/k_B T$, and this has been verified experimentally by Herweg [2]. Subsequently, it has been observed by Piekara [3] that a high field can also lead to enhanced relaxation amplitudes relative to the low field limit. This effect is now referred to as chemical effect, and it can occur when species of different dipole moments coexist in equilibrium. For observing these two effects, it is sufficient to add a high dc bias electric field to a small oscillating field whose frequency is appropriate for detecting the static dielectric constant, ε_s, as a function of the bias field [4].

The present brief review of nonlinear dielectric effects and the techniques involved focuses on the more recent recognition that high fields are also capable of modifying the dielectric relaxation times, even without changing temperature [5]. As with the field induced changes of ε_s or Δε, the value of the dielectric time constant τ_D can also change in both directions, i.e., towards both faster and slower dynamics. Figure 1 labels these four distinct effects that have been recognized thus far as nonlinear dielectric effect, and indicates the main spectral changes associated with each mechanism.

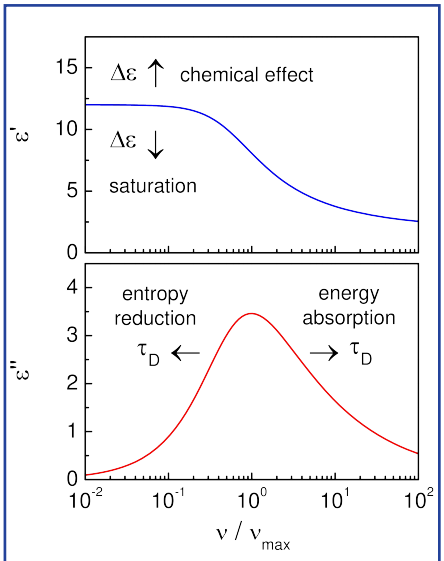

Figure 1. Schematic outline of the four recognized contributions to nonlinear dielectric effects, including their predominant impact: chemical effect increases Δε, saturation decreases Δε, energy absorption reduces τ_D, and entropy reduction increases τ_D.

There are a number of experimental challenges that need to be addressed when measuring nonlinear effects. Even when a material is subjected to an electric field that is near its breakdown field (or dielectric strength), the energy involved in the orientation of a dipole (μE) remains small compared with thermal energies ($k_B T$). Accordingly, field induced modifications of the permittivity are rather small, and very high fields are desired to obtain good resolution of the nonlinear effects. In practice, achieving high fields, $E = V/d$, is usually a combination of boosting the voltage (V) applied to the sample and employing small electrode separations (d). Usable fields are not only limited by the dielectric strength of the sample, but also by the spacer materials used and by the voltage and current capabilities of the voltage booster. In the linear response regime the voltage does not need to be constant across the entire frequency range, but nonlinear effects depend quadratically on the voltage or field and quantifying these effects thus requires a voltage that is independent of current load and frequency. Typically, this requirement restricts the frequency range of high field impedance measurements relative to the low field broadband dielectric spectroscopy. Naturally, high field requirements are more demanding when samples with small relaxation amplitude or dipole moment density are studied.

It is important to realize that both conductive and dielectric materials will absorb energy from a time dependent high amplitude electric field. For a dielectric subject to a field $E_0\sin(\omega t)$, the amount of energy density absorbed per period is $q=\frac{1}{2}\varepsilon_0 E_0^2\varepsilon''(\omega)$, while dc conductivity σ_{dc} leads to $q=\sigma_{dc}E_B^2 t$ for a dc field E_B. Because this energy will eventually end up as heat in the sample and because the amount increases linearly in time, the duration of applying the high field needs to be limited to avoid an increase of the sample temperature. Thin samples help reducing this heating effect, as thermal diffusion to the electrodes acting as heat sinks is more effective relative to electrode spacings with larger d.

There are two distinct approaches to measuring dielectric relaxation at high electric field levels, where the applied field can generally be written as $E(t) = E_B + E_0\sin(\omega t)$. One case uses a high peak field E_0 with zero bias field E_B, the other uses a high bias field E_B combined with a small alternating field $E_0\sin(\omega t)$ which itself would remain in the linear response regime. How these two approaches differ in probing the nonlinear susceptibility is indicated in Fig. 2. Regardless of whether E_B or E_0 is chosen to reach a high field level, there are different strategies to quantify how a high field modifies the dielectric relaxation behavior. One can focus on the absolute or relative change of permittivity from its low (ε_{lo}) to its high (ε_{hi}) field value, $\varepsilon_{hi} - \varepsilon_{lo}$ or $(\varepsilon_{hi}-\varepsilon_{lo})/\varepsilon_{lo}$, evaluated at the fundamental frequency ω. Alternatively, one can evaluate susceptibilities at the higher harmonics (χ_3, χ_5, etc.) by analyzing the polarization at ω_3, ω_5, and so on.

When a large amplitude field is applied to a sample, all four contributions identified in Fig. 1 may be expected to contribute to the nonlinear dielectric behavior, but with chemical effects being negligible for most simple liquids. This makes it seem impossible to study the effects individually, but by the proper field protocol (ac or dc) and by the distinct

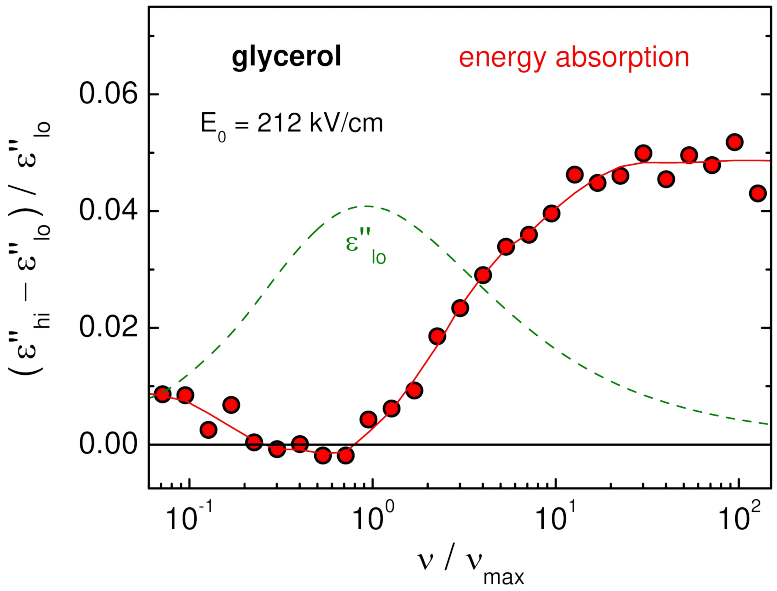

Figure 3. Effect of energy absorption from an ac field with peak value E_0 = 212 kV/cm in terms of the relative change of the dielectric loss. The dashed line outlines the loss peak, $\varepsilon''_{lo}(\omega)$, scaled arbitrarily. The data is for glycerol at T = 213 K with loss peak frequency ν_{max} = 150 Hz, taken from ref. [6].

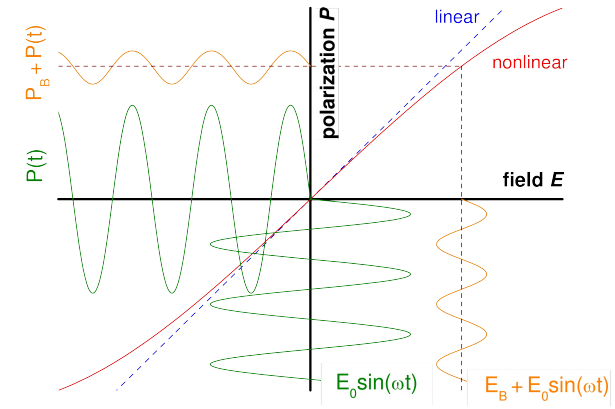

Figure 2. Linear (dashed) versus nonlinear (solid) susceptibility curve in a P versus E diagram, including the different field patterns for probing the dielectric behavior: a high ac field with no dc bias or a high dc bias field with superposed low amplitude ac field.

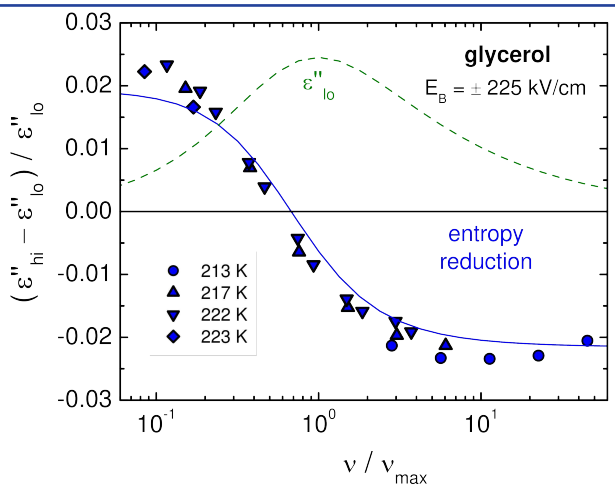

Figure 4. Effect of entropy reduction and saturation from a dc field with peak value E_B = 225 kV/cm in terms of the relative change of the dielectric loss. The dashed line outlines the loss peak, $\varepsilon''_{lo}(\omega)$, scaled arbitrarily. The data is for glycerol at the four temperature indicated, taken from ref. [7].

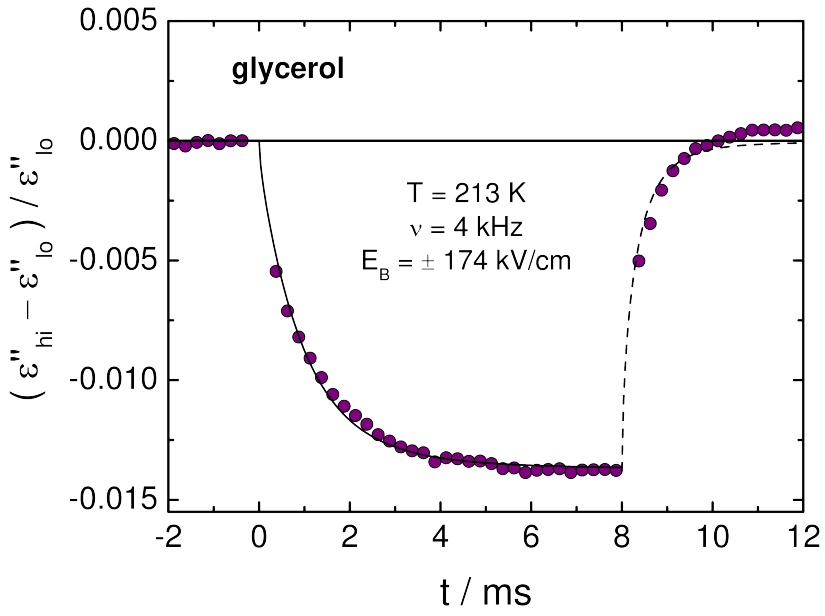

Figure 5. Time resolved reduction of the loss at a frequency of 4 kHz in response to switching a dc field of E_B = 174 kV/cm on at t = *0* and off again at t = 8 ms, reflecting the effect of both entropy reduction and saturation. The time dependence is governed by the average structural relaxation time, τ_α, and the rise/fall asymmetry is a matter of the quadratic field dependence. The data is for glycerol at T = 213 K with loss peak frequency ν_{max} = 150 Hz, taken from ref. [8].

frequency dependences, the effects can be separated to some extent. Modifications of $\Delta\varepsilon$ can be distinguished from those of τ_D by focusing on the static dielectric constant. Identifying field induced changes of dynamics requires comparing the dielectric relaxation spectrum at high and low fields across a range of frequencies. An example of the effect of energy absorption from a large ac field is shown in Fig. 3, where accelerated dynamics dominate the changes for $\nu > \nu_{max}$ [6], and the rise of ε''_{hi} for $\nu < \nu_{max}$ in Fig. 3 is likely a matter of entropy reduction (see below). A sample can absorb energy only from a time dependent field, implying that this source of reducing τ_D can be suppressed by applying high dc bias rather than ac fields. An example of such an experiment is depicted in Fig. 4, where entropy reduction and saturation effects are the main sources of nonlinear behavior [7]. Here, the relative change of ε'' clearly indicates a shift of the entire loss peak towards lower frequencies, and a saturation effect that accounts for the reduction of ε'' at its peak frequency, $\nu = \nu_{max}$.

Steady state spectra such as those of Fig. 3 and Fig. 4 can be measured with impedance equipment capable of handling high ac and dc fields. However, care has to be taken to expose the sample to the high field for a time sufficient to establish steady state, while avoiding excessive energy uptake that could lead to a change of the sample temperature. An example of a time resolved measurement at a fixed frequency ω is provided in Fig. 5, which requires recording the voltage and current traces with a digitizing oscilloscope and then performing a Fourier analysis separately for each period so that the time resolution is $\Delta t = 2\pi/\omega$ [8]. Such experiments reveal that it takes approximately the average structural relaxation time, τ_α, for the system to achieve equilibrium with the field. Accordingly, measurements at relatively high frequencies, $\nu >> \nu_{max}$, may require thousands of periods before steady state is reached.

An alternative assessment of nonlinear behavior is via the higher harmonic responses, which are completely absent in the linear response regime. The detection of these signals requires harmonic voltage sources with very low harmonic distortion, and gain/phase or lock-in type analyzers capable of analyzing higher harmonics at 3ω, 5ω, etc. for pure ac fields, and additionally at 2ω, 4ω, etc. in the presence of a high dc bias field.

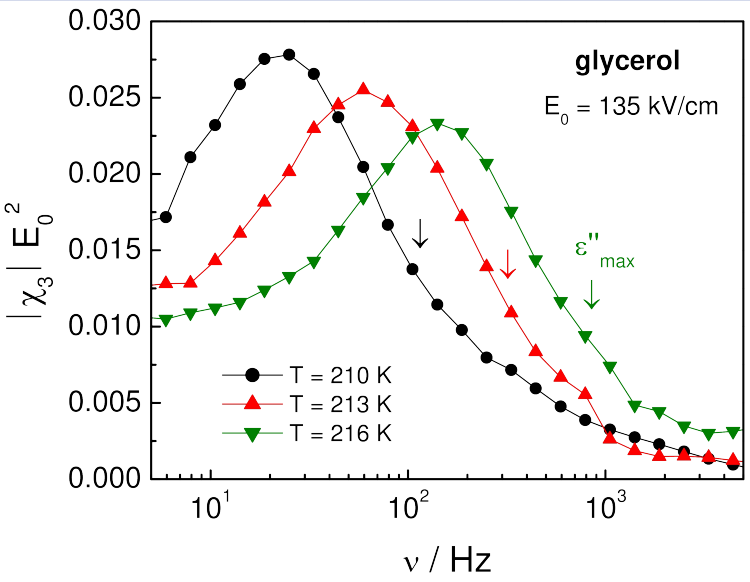

Figure 6. Spectra of the third harmonic susceptibility at three different temperatures, reported in terms of the quantity $|\chi_3|E_0^2$, based on peak fields of E_0 = 135 kV/cm. Arrows indicate the low field loss peak frequency positions, ν_{max}. The data is for glycerol at the temperatures indicated, taken from ref. [9].

Examples of third harmonic susceptibility spectra are given in Fig. 6, showing $|\chi_3|E_0^2$ curves which peak at frequencies below the low field loss peak. Here, saturation, energy absorption as well as entropy reduction have been found to contribute to χ_3 [9]. Observing higher harmonics such as χ_5 and χ_7 requires highly sensitive equipment, but such spectra have been measured [10,11].

In conclusion, present dielectric equipment is capable of measuring very small changes in permittivity or higher harmonic signals induced by high electric fields. These novel techniques provide access to dielectric features that remain absent in the low field counterparts, i.e., the sensitivity of relaxation amplitude and time scale to the electric field. Moreover, time resolved methods can follow the equilibration process with the high field, analogous to physical aging.

References

[1] R. Richert, Adv. Chem. Phys. 156, 101 (2014).
[2] P. Debye, Polar Molecules (Chemical Catalog Company, New York, 1929).
[3] A. Piekara and B. Piekara, Compt. Rend. Acad. Sci. (Paris) 203, 852 (1936).
[4] S.J. Rzoska and V.P. Zheleznny (eds), Nonlinear Dielectric Phenomena in Complex Liquids (Kluwer Academic Publishers, Dordrennnnncht, 2004).
[5] R. Richert, J. Phys.: Condens. Matter 29, 363001 (2017).
[6] R. Richert and S. Weinstein, Phys. Rev. Lett. 97, 095703 (2006).
[7] S. Samanta and R. Richert, J. Chem. Phys. 142, 044504 (2015).
[8] A.R. Young-Gonzales, S. Samanta, and R. Richert, J. Chem. Phys. 143, 104504 (2015).
[9] P. Kim, A.R. Young-Gonzales, and R. Richert, J. Chem. Phys. 145, 064510 (2016).
[10] S. Albert, T. Bauer, M. Michl, G. Biroli, J.-P. Bouchaud, A. Loidl, P. Lunkenheimer, R. Tourbot, C. Wiertel-Gasquet, and F. Ladieu, Science 352, 1308 (2016).
[11] L.N. Patro, O. Burghaus, and B. Roling, Phys. Rev. Lett. 116, 185901 (2016).

Ranko Richert
School of Molecular Sciences
Arizona State University
Tempe, AZ 85287-1604, U.S.A.
email: ranko@asu.edu

Advanced low frequency liquid sample holder: double guard electrodes

A. Greenbaum (Gutina), I. Popov, V. Lirtsman and Yu. Feldman

Introduction

Broadband dielectric measurements on liquid samples over wide temperature intervals are not an easy task for many years [1,2]. The traditional sample cell, based on the use of a parallel-plate capacitor, does not meet many requirements for the investigation of liquids.

A couple of years ago, a cylidrical three-electrode cell configuration has been suggested [3] with the objective of improving the reliability and repeatability of dielectric studies of liquids and their mixtures. That cell was offered by Novocontrol as “BDS 1307 liquid cylindrical sample cell”.

In this contribution, we suggest an advanced version of this sample cell configuration based on a double guard electrodes system, allowing complex dielectric permittivity measurements of liquids in various thermodynamic states. Compared to traditional two- or simple three-electrode cylindrical liquid sample cells, the new design drastically reduces edge effects, resulting in significantly improved measurement accuracy.

Configuration of the double guard electrodes sample holder

Figure 1 shows the schematic cross section of the double guard electrodes liquid cell. This particular cell configuration suppresses errors due to the thermal expansion of a measured liquid, protects against sample leakage and prevents evaporation. The design is based on a cylindrical stainless steel capacitor that allows the dielectric measurements of the liquid under dynamic conditions, even with fast cooling or heating rates. The capacitor is filled up to the center level of the upper guard electrode. Leaving a small empty volume at the top prevents liquid pressure from changing. The measurement cell is then sandwiched

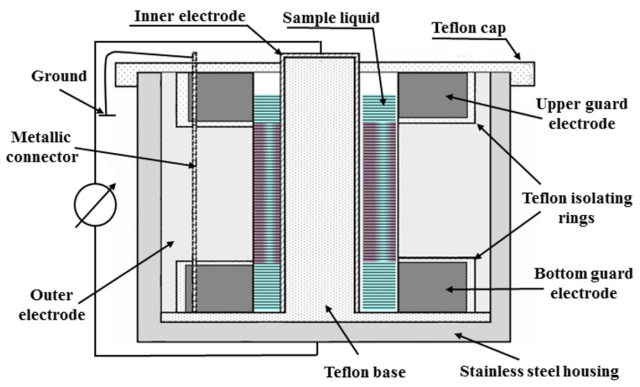

Figure 1. Schematic cross section of the new double guard electrodes cell. The center of the upper guard electrode marks the filling height of the liquid (blue shading), varying with temperature due to thermal expansion. The effective region for the dielectric measurement is marked by the red gradient. The Teflon cap prevents both pollution of the liquid sample from the environment and fast evaporation of the liquid.

between the parallel-plate electrodes of the regular Novocontrol sample holder for dielectric measurements in the frequency range below 3MHz. 3D projections of the disassembled cell and a photograph of the assembled cell are presented in Figure 2.

The assembled cell should be mounted into the standard sample cell of the Novocontrol setup while connecting the guard electrodes to the grounded terminal of the Novocontrol holder (see Figure 3).

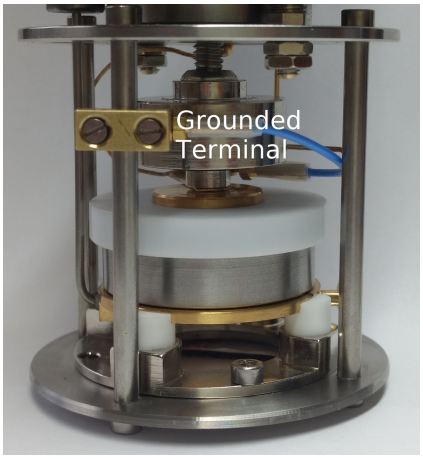

Figure 3. The liquid sample cell mounted into the standard Novocontrol sample cell.

Advantages of the double guard electrodes liquid sample holder

The suggested new design of the cylindrical liquid sample holder exhibits several considerable advantages over the previous three-electrode model [3]:

- *The effective homogeneous electric field is confined to a constant liquid volume, removing parasitic edge effects*
  Suppressing contributions to the measured capacitance due to external cell elements (stray capacity) significantly increases the reliability and reproducibility of the dielectric measurement.
- *Adding a second guard electrode creates a symmetric testing volume from the electrical point of view*
  The fringing field effect is minimized by modifying the cell design towards higher symmetry. Residual small effects can be removed by a simple calibration procedure performed prior to the dielectric measurement.
- *Several Teflon-metal screwed connections are removed; only metallic parts are screwed to each other*
  Compared to stainless steel, Teflon is a very soft material. Removing Teflon-metal screw connections enhances the durability of the Teflon sample cell elements and thus increases the overal fixture lifetime. Additional effects are higher cell stability and measurement reproducibility.
- *Simplified sample cell assembling/ disassembling*
  The simplicity of cell assembling/ disassembling is a key parameter for high-throughput experiments of a set of varying liquids. User-friendly and quick sample holder handling allows reproducible results after only little training and saves time and effort.
- *Increase of the Empty Cell Capacitance*
  The increased geometrical empty cell capacitance of almost 1.3 pF allows measuring low permittivity liquids with improved accuracy.
- *Unique cell structure prevents leakage of the liquid between cell elements*
  The leakage of the liquid between cells elements leads to changes of the parasitic capacity as a function of the external thermodynamic parameter. The unique new double guard electrodes structure results in a stray capacity which remains unchanged during the entire experiment. Furthermore, the tight lock of the structural elements prevents appearance of air bubbles in the volume under study. This leads to an extremely high reproducibility of the measurements.
- *Calibration procedure reduced to a single open cell measurement*
  Calibration measurements of standard liquids (necessary in the previous design) is no longer required.

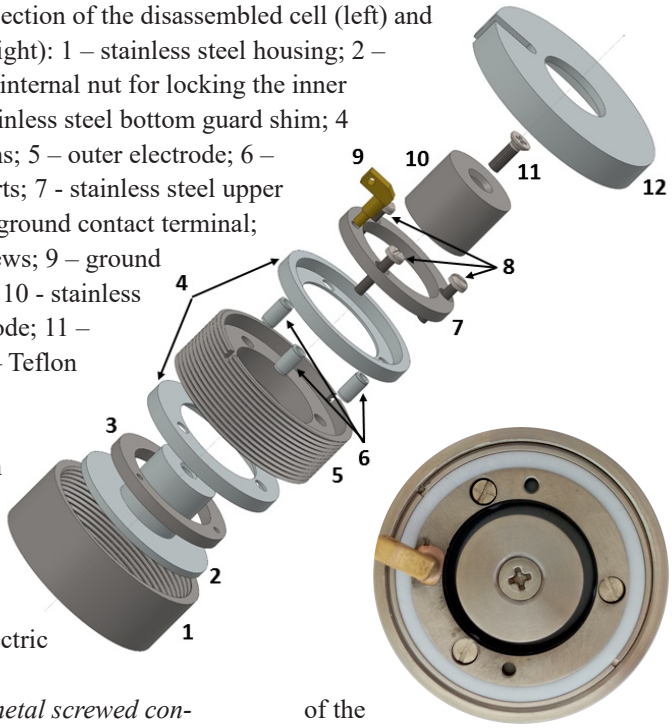

Figure 2. 3D projection of the disassembled cell (left) and assembled cell (right): 1 – stainless steel housing; 2 – Teflon base with internal nut for locking the inner electrode; 3 – stainless steel bottom guard shim; 4 – two teflon shims; 5 – outer electrode; 6 – three Teflon inserts; 7 - stainless steel upper guard shim with ground contact terminal; 8 – three M2 screws; 9 – ground contact terminal; 10 - stainless steel inner electrode; 11 – M2.5 screw; 12 – Teflon cap.

Calibration procedure

For entry into the WinDETA Sample Specification dialogue, dimensional parameters equivalent to a parallel-plate capacitor setup (diameter, thickness, stray capacity) are delivered along with the sample cell.

To improve the accuracy of the measurements it is strongly recommended to calibrate the cell prior to the experiment.

The capacity of an empty cylindrical capacitance C_0 is given by

$$C_0 = 2\pi\varepsilon_0 L/\ln(b/a). \quad (1)$$

Here, ε_0 is the vacuum dielectric permittivity; L – height of the outer

electrode of the cylindrical cell; *b* and *a* – diameters of the outer and inner electrodes, respectively.

The measured capacity, (C_p' in WinDeta) of the empty clean cell can be represented as follows:

$$C_p' = \varepsilon_{mair} \cdot C_0 = \varepsilon_{air} \cdot C_0 + C_{add}, \quad (2)$$

where ε_{mair} is the measured static dielectric permittivity of air, ε_{air} the known static dielectric permittivity of air. The additional capacity C_{add} is in parallel to the sample capacity, remaining constant for any measurements and contributing to the real part of the complex capacity only. Performing such test measurement and taking into account that ε_{air}=1, we obtain C_{add} as

$$C_{add} = C_p' - C_0. \quad (3)$$

The calculated value of C_{add} should be placed into the WinDETA entry area labelled

Cell Stray + Spacer Capacity [pF]

of the Sample Specification dialogue.

An example of the application of the double guard electrodes liquid sample cell for the measurement of pure glycerol is presented in Figure 4. The main relaxation process, dc conductivity and high frequency excess wing are clearly observed.

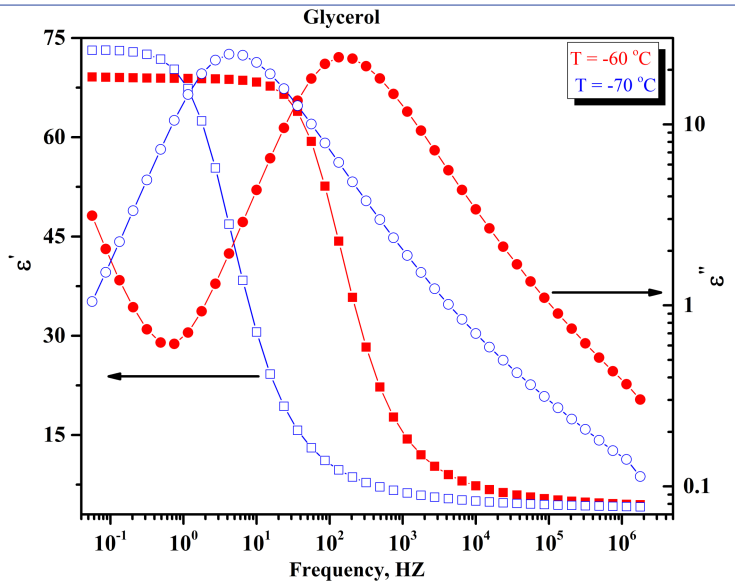

Figure 4. The frequency behavior of the dielectric losses of pure glycerol at two different temperatures.

References

[1] U. Kaatze, R. Feldman, P. Ben Ishai, A. Greenbaum (Gutina), and V. Raicu, "Experimental Methods," in Dielectric Relaxation in Biological Systems, Oxford: Oxford University Press, 2015.

[2] A. Greenbaum (Gutina), P. Ben Ishai, and Y. Feldman, "Analysis of Experimental Data and Fitting Problems," in Dielectric Relaxation in Biological Systems, Oxford: Oxford University Press, 2015.

[3] Y. Hayashi, A. Gutina and Yu. Feldman, Dielectric Newsletter, 21, 6-7 (2005).

A. Greenbaum (Gutina)[1,2], I. Popov[1], V. Lirtsma[1] and Yu. Feldman[1]
The Hebrew University of Jerusalem
[1]Department of Applied Physics
[2]Racah Institute of Physics
Jerusalem, Israel.
Email: Anechka@mail.huji.ac.il

The Next Generation Dielectric Analyzer: Alpha-A Rev. C

Dirk Wilmer

Introduction

When the first Novocontrol broadband dielectric/impedance analyzers were introduced in 1999, they were soon accepted by researchers in physics, chemistry, biology, materials science and various other fields[1]. These devices exhibited an extremely wide impedance range (from 10 mΩ to beyond 100 TΩ) and allowed accurate loss measurements with unsurpassed tan δ accuracy (better than $3 \cdot 10^{-5}$) and resolution (better than 10^{-5}).

The Novocontrol analyzers made the entire impededance range accessible in one single set-up, i.e., without any need to change the hardware configuration to accomodate different parts of the impedance range. This property is essential for materials characterisations over wide temperature ranges: here many materials change from insulating to conductive, and only impedance analysis systems covering the entire impedance range allow fully automatic measurements, e.g., as a function of frequency and temperature.

We are proud to announce our next generation of top-class broadband dielectric analyzers, the Alpha-A Rev. C series which, in spite of its basically unchanged exterior, was widely modified inside: it comes with a new microprocessor control unit, faster and more precise analog/digital converters, a new ac voltage signal generator plus newly designed voltage inputs channels. The new hardware addresses two objectives: improved performance and new measurement options (extended functionality).

Improved overall performance

The new Alpha-A analyzer provides a total of thirteen voltage input ranges (increased by four), with values from 45 mVp to 45Vp (four voltage ranges per voltage decade). This extension improves detection of small ac signals in the presence of large dc contributions and allows to perform dc coupled impedance measurements

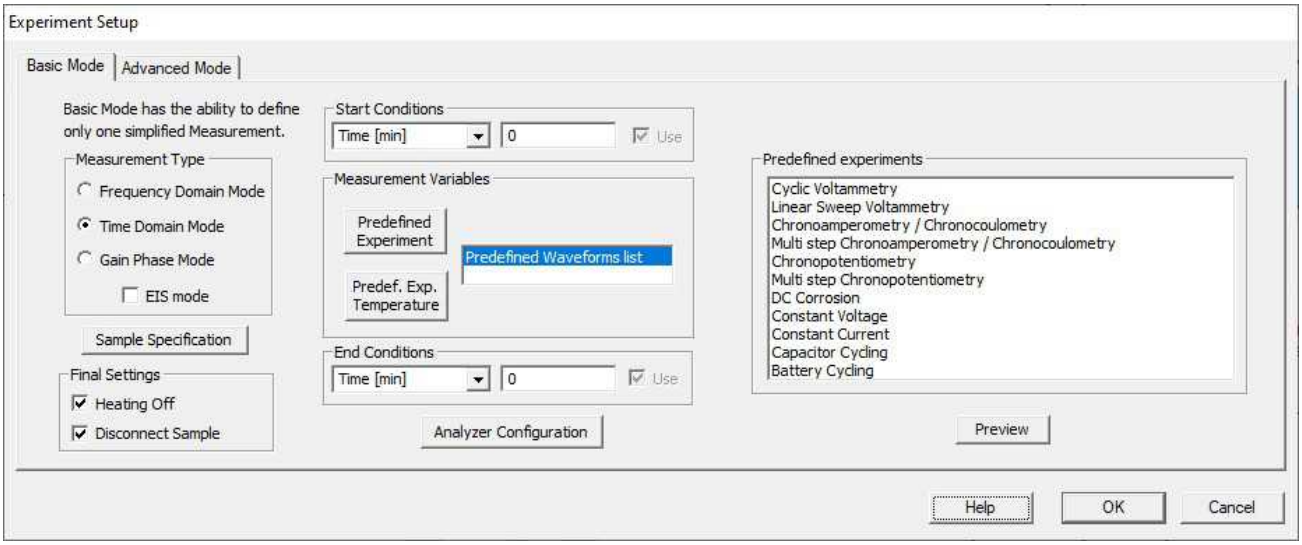

Figure 1: Time Domain Experiment Setup (DETACHEM Basic Mode). Easy access and setup for pre-defined experiments.

over the entire range of dc bias even for the standard test interfaces ZG2 and ZGS.

The new Alpha-A signal generator provides a built-in dc bias capability—it allows to select a mixed ac/dc signal up to 4.5 Vp. The new dc bias function exhibits improved resolution and accuracy (1 mV and 10 mV, respectively).

The signal generator and voltage input channels may be extended for operation at frequencies beyond 100 MHz. To this end, however, cabling, sample cells, test interfaces and their calibrations require additional development to render such feature usable for a wider range of applications.

Finally, the overall accuracy has improved by a factor of three at high frequencies. Between 100 Hz and 100 kHz, the tan δ precision improved by a factor of three. Measurement speed has increased to a new maximum of about 600 impedance points per second.

Nonlinear broadband dielectric and conductivity spectroscopy - Improvements for measuring higher harmonics

Non-linear behaviour is the electric field dependence of electrical materials parameters like permittivity ε, susceptibility $\chi = \varepsilon - 1$, or conductivity σ. It is visible either directly in the field dependence of these parameters or in the study of the contribution of higher harmonics. Access to these effects requires suitable high-field generators and measurement devices [2]. In spite of the higher demand on equipment and data analysis required for studies of non-linear behaviour of materials, the number of important publications has increased recently [3-9].

The option to study non-linear behaviour of materials has already been supported by earlier revisions of the Alpha-A analyzer. There were some restrictions though: at frequencies above 1.5 kHz, e.g., harmonics were only available as moduli, there was no phase information available.

Rev. C of the Alpha-A, however, delivers real and imaginary parts of higher harmonics and thus the corresponding phase angles over the entire accessible frequency range.

The performance of higher harmonics measurements is severely improved at frequencies below 1 kHz. The new design reduces the contribution of higher harmonics of the generator voltage from 10^{-3} (-60 dB) to $2 \cdot 10^{-5}$ (ca. -90 dB), thereby improving the measurement accuracy by a similar amount. Such improvement is particularly important as the higher harmonics signals by their very nature are small and thus go easily undetected if noise levels are too high. Highly sensitive equipment, however, even allowed determination of higher harmonics like χ_5 and χ_7 [4, 10].

Extended functionality: Time Domain

For earlier revisions of the Alpha-A, time domain measurements were restricted to configurations using our POT/GAL electrochemical test stations. For Rev. C., measurements in the time domain are feasible in all test interface configurations, including those using the standard test interfaces (ZGS, ZG2, ZG4) and the high-voltage boosters (HVB300, HVB1000, HVB4000). This extension of hardware possibilities is complete-mented by full support through the DETACHEM software which allows a much wider range of experiments in both time and frequency domains and multi-experiments which may constitute combinations thereof, see below.

The new Alpha-A Rev. C allows time-domain measurements with arbitrary waveform signals. This means that the experimentalist is free to define all sorts of voltage or current signals as a function of time, e.g, ramps, pulses, sinusoidal, chirp, and measure the corresponding material or devices response signal (current or voltage, respectively). In this operational mode, the smallest definable

time step is 100 ns.

The time domain measurements described here are not designed to provide access to impedance or permittivity spectra via Fourier transforms—such transforms would, in general, provide results of much less precision and accuracy than direct impedance measurements in the frequency domain.

Example materials for investigations using both time and frequency domain methods are

- Supercapacitors (determination of capacity and ESR)
- High-performance industrial dielectric foils
- Batteries, fuel cells and their components.

References

[1] G. Schaumburg, Dielectrics Newsletter, May 1999.
[2] R. Richert, Dielectrics Newsletter, this issue.
[3] Richert, R (ed.), Nonlinear Dielectric Spectroscopy, Springer International Publishing, 2018.
[4] Albert, S., Bauer, T., Michl, M., Biroli, G., Bouchaud, J.P., Loidl, A., Lunkenheimer, P., Tourbot, R., Wiertel-Gasquet, C. & Ladieu, F. 2016. Science 352 (2016) 1308.
[5] Michl, M., Bauer, T., Lunkenheimer, P. & Loidl, A. 2014. Phys. Rev. Lett. 114, 067601 (2015)
[6] Bauer, T., Lunkenheimer, P., Kastner, S. & Loidl, A. 2013. Phys. Rev. Lett. 110:107603.
[7] Bauer, T., Michl, M., Lunkenheimer, P., Loidl, A., J. Noncryst. Solids 407:66.
[8] Michl, M., Bauer, T., Lunkenheimer, P. & Loidl, A. 2015. J. Chem. Phys. 144 (2016) 114506.
[9] Casalini, R., Fragiadakis, D. & Roland, C.M. 2015. Journal of Chemical Physics 142:064504.
[10] Patro, L. N.; Burghaus, O. & Roling, B., Phys. Rev. Lett., American Physical Society, 2016, 116, 185901.

DETACHEM - unified software for measurement, control, and visualisation in frequency and time domains

Dirk Wilmer

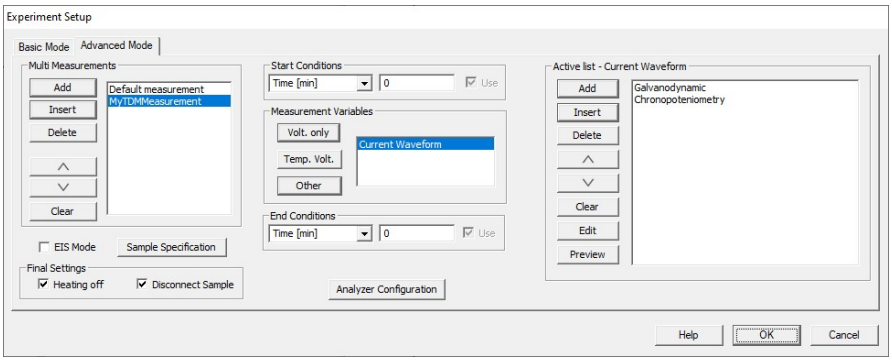

DETACHEM is our new unified control and evaluation software for dielectric and electrochemical impedance spectroscopy as well as time domain measurements (dc voltage/current). It further allows gain-phase and magnetic measurements. DETACHEM provides a uniform user interface nearly independent of the particular hardware, supporting the most important dielectric or impedance analyzers and temperature controllers.

DETACHEM automatically performs the calibration procedures for the sample cells and allows dielectric and impedance measurements up to four dimensions as a function of frequency, temperature, time, ac voltage or dc bias or any multi dimensional combination.

The basic frequency and time domain parameters like dielectric function, modulus, conductivity, impedance, voltage, current etc. are evaluated and displayed graphically in two and three dimensional representation.

Basic Mode

The Basic Mode of DETACHEM allows quick and easy configuration of standard experiments. Time domain configurations, e.g., are selected from a list of predefined experiments with parameters entered in self-explanatory graphical menus. Examples are cyclic voltammetry, linear sweep voltammetry, square wave voltammetry, chronoamperometry/chronocoulometry, chronopotentiometry, pulsed and stepped methods, dc corrosion, constant voltage or current, battery and capacitor cycling.

Advanced Mode

Advanced Mode offers much more complex experimental configurations. It allows to run measurements of different modes (frequency domain, time domain, gain-phase) to be set-up to run sequentially. Further options include grouping of measurement steps and repeating both single measurements and groups of measurements. Self-defined measurements can be reused by referring to their name. While the DETACHEM Basic Mode represents the ideal entry point for beginners and also for routine experiments, the Advanced Mode provides a myriad of new possibilities. Since it is possible, e.g., to use the standard experiments of time domain mode in Advanced Mode as well, the Advanced Mode can be considered as highly sophisticated extension of the basic mode for more complex situations.

novocontrol technologies
Novocontrol Technologies
GmbH & Co. KG
Aubachstr. 1
56410 Montabaur
Germany
Phone: +49 2602 9196690
Fax: +49 2602 91966933
e-mail: novo@novocontrol.de
web: http://www.novocontrol.de